LETTER

doi:10.1038/nature10391

Transcriptomic analysis of avian digits reveals conserved and derived digit identities in birds

Zhe Wang[1], Rebecca L. Young[1], Huiling Xue[2] & Günter P. Wagner[1]

Morphological characters are the result of developmental gene expression. The identity of a character is ultimately grounded in the gene regulatory network directing development and thus whole-genome gene expression data can provide evidence about character identity. This approach has been successfully used to assess cell-type identity[1–3]. Here we use transcriptomic data to address a long-standing uncertainty in evolutionary biology, the identity of avian wing digits[4,5]. Embryological evidence clearly identifies the three wing digits as developing from digit positions 2, 3 and 4 (ref. 6), whereas palaeontological data suggest that they are digits I, II and III[7]. We compare the transcriptomes of the wing and foot digits and find a strong signal that unites the first wing digit with the first foot digit, even though the first wing digit develops from embryological position 2. Interestingly, our transcriptomic data of the posterior digits show a higher degree of differentiation among forelimb digits compared with hindlimb digits. These data show that in the stem lineage of birds the first digit underwent a translocation from digit position 1 to position 2, and further indicate that the posterior wing digits have unique identities contrary to any model of avian digit identity proposed so far[5,8].

To address the problem of avian digit identity we performed mRNA-seq analysis from pools of 40 individually isolated chicken forelimb and hindlimb digits at two stages of development: stages 28/29 and 31 (Fig. 1a–d). A total of 14,692 annotated genes was detected and compared among samples. Sampling pools of populations are highly reproducible (Supplementary Fig. 1). In describing the results we distinguish nominal digit identities, based on position, from biological digit identities; that is, those that indicate homologies. Nominal digit identities use a three-letter code, the first giving developmental stage (E, early for stage 28/29; L, late for stage 31) and the second giving limb identity (F, forelimb; H, hindlimb). The two letters are followed by a lowercase letter giving the anterior–posterior location of chondrified digits, with 'a' for the most anterior digit and 'b', 'c' and 'd' for the posterior digits. In contrast, biological digit identities (homologies) are indicated by roman numerals I, II, III and IV. Finally, embryonic digit positions are indicated with Arabic numerals from anterior to posterior: 1, 2, and so on. These terminological differences are necessary to distinguish descriptive references to certain digits in the adult hand (a, b, etc.) from statements about embryological digit positions (1, 2, etc.) and biological digit identity or homology (digits I, II, etc.).

Transcriptomic data have not been systematically applied to address questions of digit homology. At the most general level, the transcriptome is a phenotypic character and is thus a legitimate source of evidence regarding character identity. Gene expression data from a limited number of genes have successfully been applied to questions of homology in the past[9–11]. Cell-type identity is another area where gene expression has proven to be valuable[12–14]. Here we refer to homology as the historical continuity of the developmental programme that determines developmental individuality of the character. By this definition, homology is thus tied to continuity in the expression of regulatory genes[15,16].

First we performed a multidimensional scaling (MDS) analysis[17] to identify the overall similarity structure of the transcriptomes (Fig. 1e). After removing the effect of forelimb–hindlimb differences—that is, removing differentially expressed genes between forelimb and hindlimb—the ordination analysis reveals four clearly resolved clusters corresponding to early and late anterior digit clusters, and two clusters of early and late posterior digits. The transcriptomic data thus contain two strong signals: one pertaining to the difference between the first digits and the posterior digits, and the other reflecting developmental stages.

The heat map of correlation coefficients between samples and hierarchical clustering analyses based on the expression of all detected genes also give strong support for a cluster of anterior digits (Fig. 1f and Supplementary Fig. 2). These data indicate that the anterior digits in the wing and the hindlimb are homologous (Fa = Ha). There is broad agreement that the anterior-most digit in the chicken foot is homologous to digit I in the ancestral five-digited limb of crown-group tetrapods (Ha = DI). We conclude that the most anterior digit in the wing is likely to be homologous to digit I. The transcriptomic data are consistent with the morphological data that show a continuity of digit I identity along the theropod lineage[7].

The existence of a cluster that unites the forelimb and hindlimb digits I is significant because the first forelimb digit in the chick develops from the embryonic position that normally develops into digit II, that is, Fa develops from embryonic position F2 whereas Ha develops from embryonic position H1 (ref. 18). The difference between the digit I cluster and the posterior digits could reflect the posterior to anterior gradient in digit development[19]. However, the separation of the anterior digit I cluster is also found in stage 31, where the anterior and the posterior digits are at comparable levels of differentiation (compare Fig. 1c, d). To analyse which genes are driving the digit I cluster, we identified 556 significantly differentially expressed genes between digit I and the other digits (Supplementary Fig. 3). Gene Ontology (GO) analysis of these differentially expressed genes detected seven enriched GO terms of molecular function and biological process. Transcription factor activity is the top GO term, indicating that the transcriptome data sort digits according to their gene regulatory signature (Supplementary Table 1). Other over-represented GO terms are DNA binding, regulation of transcription, and skeletal system development. These results indicate that the distinction between the first digits and the rest of the digits reflects the developmental individuality of digit I relative to the posterior digits; that is, Fa and Ha are biologically equivalent or true homologues, as suggested by palaeontological[7] and *in situ* hybridization (ISH) studies[20–22]. This result suggests that, in the theropod hand, the embryological position of digit I has changed from position 1, as in the ancestor of amniotes, to position 2 in the stem lineage of birds, consistent with the frame shift hypothesis of avian digit identity[7].

To gain more insight into the genetic nature of digit I identity we searched for digit I markers and identified *Hoxd12*, *Hand2*, *Zic3* and

[1]Yale Systems Biology Institute, and Department of Ecology and Evolutionary Biology, Yale University, West Haven, Connecticut 06516, USA. [2]Department of Genetics, Yale University School of Medicine, New Haven, Connecticut 06510, USA.

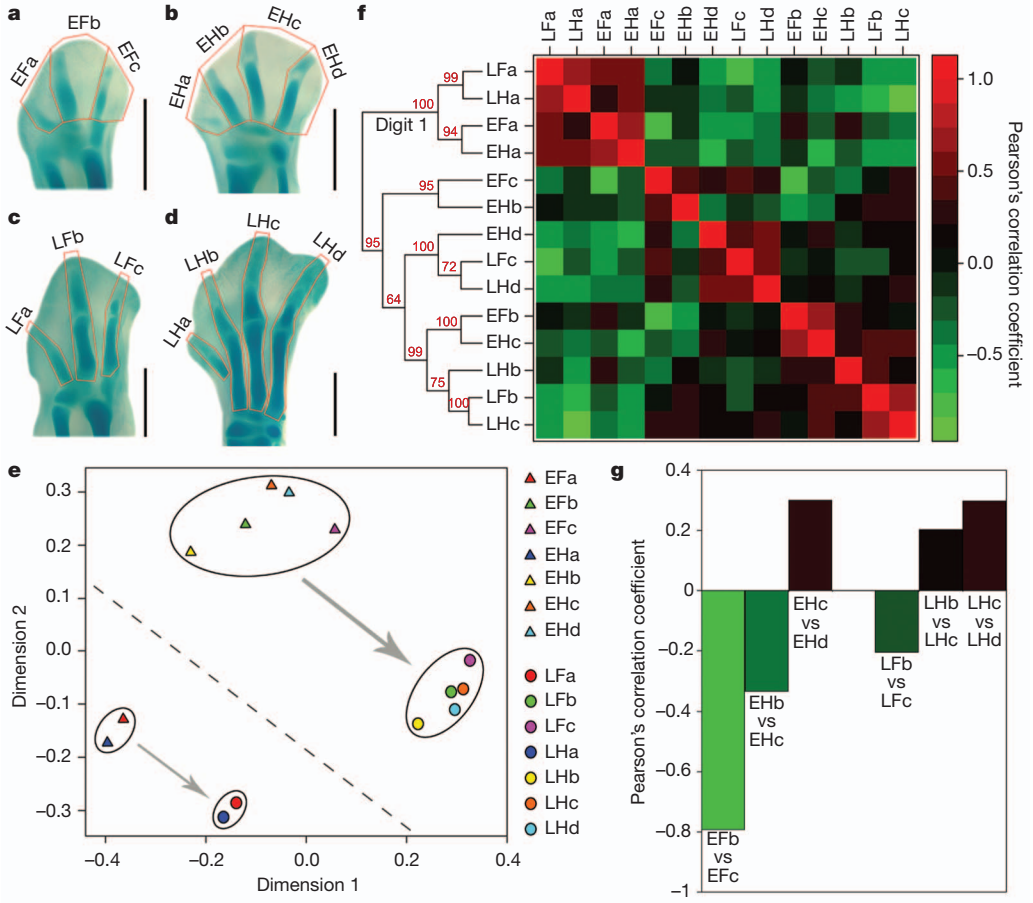

Figure 1 | Chicken embryonic digit transcriptomes identify forelimb and hindlimb digits I but no clear correspondence between posterior forelimbs and hindlimbs. **a**–**d**, Alcian-blue-stained autopods. Red lines indicate the dissection protocol used to obtain the samples for the RNA-seq analysis. Scale bar, 1 mm. **a**, **b**, Stage 28; **c**, **d**, stage 31. **e**, Ordination of transcriptome similarity, after removing forelimb–hindlimb signals. **f**, Heat map of Pearson's correlation and cluster analysis. Red numbers at the nodes represent approximately unbiased bootstrap values. **g**, Comparison between posterior forelimb digits and between neighbouring posterior hindlimb digits by Pearson's correlation coefficients.

Lhx9. *Hoxd12* and *Hand2* are well known negative markers of the anterior-most digit[20,23,24] (Supplementary Figs 4 and 5 and Supplementary Discussion). We found two novel positive markers of digit I: *Zic3* and *Lhx9* (Figs 2 and Supplementary Fig. 6).

Zic3 is always expressed more strongly in the first digit than the posterior digits, in particular at stages 26 and 28 (Fig. 2). Zic3 is a transcriptional co-factor that physically interacts with Gli3, which is important in the transduction of the Shh signal[25]. Digit I has been proposed to be refractory to Shh signalling[19], and the interaction of Zic3 protein with Gli3 may have an involvement in this (Supplementary Discussion). Lhx9 is a LIM homeodomain transcription factor that controls three-dimensional limb patterning in mouse[26] (Supplementary Discussion).

The similarity analysis of digit transcriptomes presented above does not determine to which hindlimb digits the second and third wing digits correspond. The inspection of the cluster analysis and the correlation coefficients show a pattern of conflicting signals (Fig. 1f and Supplementary Fig. 7). There are two well supported clusters that unite the second wing digit with the third hindlimb digit, (EFb, EHc) and (LFb, LHc), but these two clusters are united with the late second hindlimb digit, LHb. There is a cluster (EHd, LHd, LFc) that is indicative of the third digit in the wing having an affinity to the fourth hindlimb, but there is also a cluster that unites the early third forelimb digit with the early second hindlimb digit (EFc, EHb), indicating an incoherent signal. To identify the source of this ambiguity we propose that the degree of differentiation among the posterior digits might differ between forelimbs and hindlimbs.

To test this possibility we inspected the correlation coefficients between the posterior digits within each limb (Fig. 1g). In the early digit samples there is a strong negative correlation between the second and third wing digits but a weaker negative correlation between the second and third hindlimb digits and a positive correlation between the third and fourth hindlimb digits. In the late samples, the correlation between the second and third wing digits is still negative although weaker than for the early samples, whereas the correlations between the neighbouring posterior hindlimb digits are both positive. Together, these data indicate a much weaker differentiation between neighbouring posterior hindlimb digits than that between the posterior forelimb digits. We also performed differential expression analysis showing that the differences between posterior forelimb digits are larger than the difference between neighbouring posterior hindlimb digits (Supplementary Fig. 8). Overall, these results suggest that the second and third wing digits diverged and may have acquired derived digit identities during theropod evolution, making it difficult to find corresponding digit identities in the hindlimb.

To discover genes that specifically contribute to the second and third wing digit identities, we performed differential expression analysis of the mRNA-seq data between samples LFb and LFc. We found two genes, *Tbx3* and *Socs2*, with high expression in sample LFc (Supplementary Fig. 9 and Fig. 3a). To our knowledge no studies have been published indicating a role for *Socs2* in limb development. ISH confirms its strong expression in the third forelimb digit to the exclusion of all other digits in forelimb and hindlimb (Fig. 3b–g). Recently it has been shown that the third forelimb digit has a unique mode of

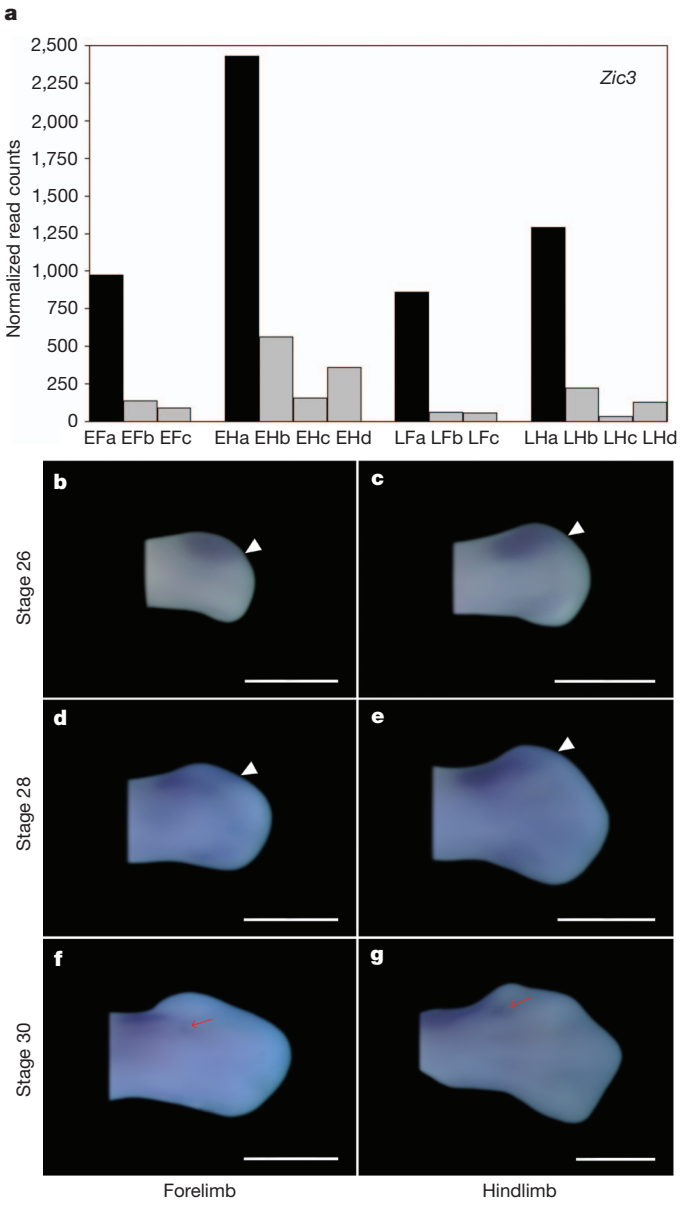

Figure 2 | Expression of *Zic3*. **a**, Expression pattern of *Zic3* in mRNA-seq samples. The *y* axis is the trimmed mean of M-values (TMM)[30] normalized mRNA-seq read-count value. **b**–**g**, Expression of *Zic3* in forelimb and hindlimb buds visualized by ISH. **b**, **c**, Stage 26; **d**, **e**, stage 28; **f**, **g**, stage 30. The dorsal view of the autopod is shown with anterior up and distal to the right. The white arrowheads in **b**–**e** indicate the expression boundary between first and second digit. The red arrows in **f**, **g** indicate the proximal expression of *Zic3*. Scale bar, 1 mm.

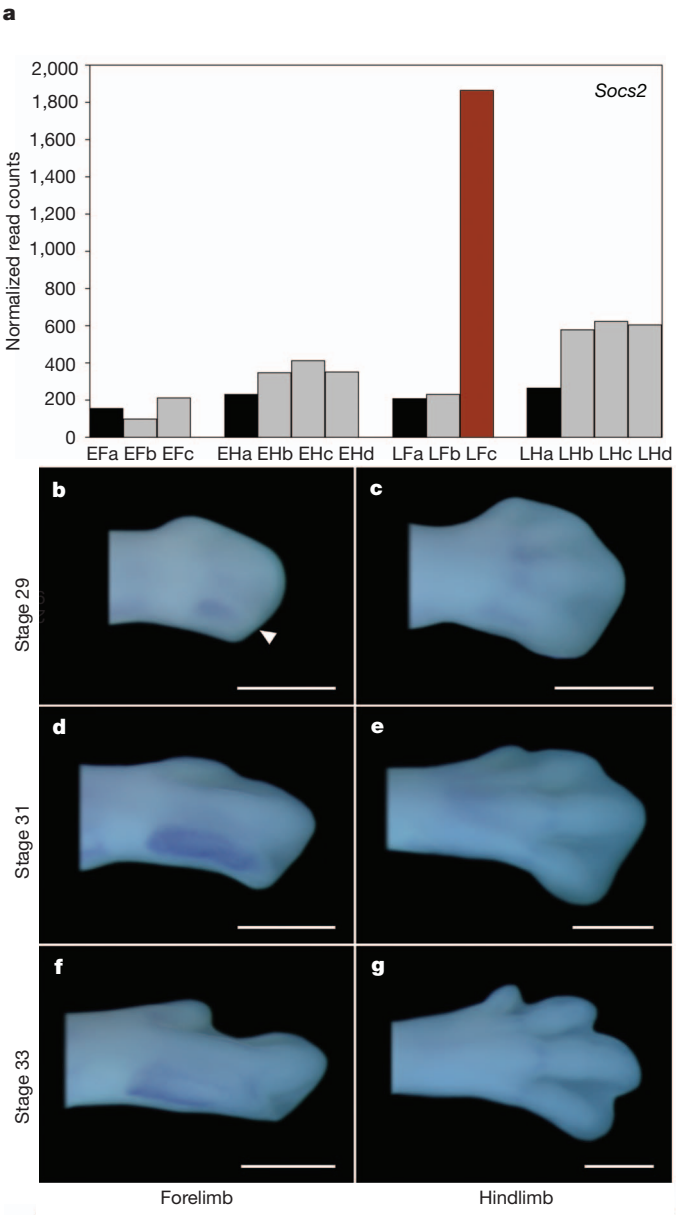

Figure 3 | Expression of *Socs2*. **a**, Expression pattern of *Socs2* in mRNA-seq samples. The *y* axis is the TMM normalized mRNA-seq read-count value. **b**–**g**, Expression of *Socs2* in forelimb and hindlimb digits visualized by ISH. **b**, **c**, Stage 29; **d**, **e**, stage 31; **f**, **g**, stage 33. Orientation of limb buds as in Fig. 2. The white arrowhead in **b** points at the expression domain at the third digit. Scale bar, 1 mm.

development in birds[8]. This, combined with our gene expression survey, supports the idea that the third wing digit has a unique derived identity in birds.

The data presented here reveal two patterns. First, there is a strong signal that identifies the anterior-most digits in the forelimb and hindlimb as homologous, in spite of the fact that they develop in different embryological positions. The second pattern is that no clear correspondence was found between the posterior forelimb digits and the posterior hindlimb digits. A comparison of digits within each limb shows that the posterior forelimb digits are more strongly differentiated than the posterior hindlimb digits, and forelimb digit III exhibits a unique expression of *Socs2* (Fig. 3d, f and Supplementary Fig. 10). These results provide evidence that the second and third wing digits are developmentally distinct from the second to fourth hindlimb digits, indicating that digit individualization can be dynamic and evolutionarily transient.

METHODS SUMMARY

Fourteen samples and two pools of twenty individuals from embryonic chicken digits were used to perform mRNA-seq on an Illumina Genome Analyzer. Digital primordia with their closely posterior interdigital mesoderm were dissected separately from the forelimbs and hindlimbs between stages 28 and 29 (stage 28/29; Fig. 1a, b). Digital rays without the interdigital tissues were collected from the forelimbs and hindlimbs at stage 31 (Fig. 1c, d). mRNA-seq data were used for clustering[17,27], correlation analysis, differential gene expression[28] and Gene Ontology analysis. For ISH, we followed a previously published protocol[29]. All the probes are labelled with digoxigenin (Roche, catalogue no. 11277073910) and hybridized with the chicken embryos at 70 °C.

Full Methods and any associated references are available in the online version of the paper at www.nature.com/nature.

Received 21 March; accepted 26 July 2011.
Published online 4 September 2011.

1. Novershtern, N. *et al.* Densely interconnected transcriptional circuits control cell states in human hematopoiesis. *Cell* **144,** 296–309 (2011).
2. Cherbas, L. *et al.* The transcriptional diversity of 25 *Drosophila* cell lines. *Genome Res.* **21,** 301–314 (2011).
3. Alizadeh, A. A. *et al.* Distinct types of diffuse large B-cell lymphoma identified by gene expression profiling. *Nature* **403,** 503–511 (2000).
4. Wagner, G. P. The developmental evolution of avian digit homology: an update. *Theory Biosci.* **124,** 165–183 (2005).
5. Young, R. L., Bever, G. S., Wang, Z. & Wagner, G. P. Identity of the avian wing digits: problems resolved and unsolved. *Dev. Dyn.* **240,** 1042–1053 (2011).
6. Burke, A. C. & Feduccia, A. Developmental patterns and the identification of homologies in the avian hand. *Science* **278,** 666–668 (1997).
7. Wagner, G. P. & Gauthier, J. A. 1,2,3 = 2,3,4: a solution to the problem of the homology of the digits in the avian hand. *Proc. Natl Acad. Sci. USA* **96,** 5111–5116 (1999).
8. Tamura, K. *et al.* Embryological evidence identifies wing digits in birds as digits 1, 2, and 3. *Science* **331,** 753–757 (2011).
9. Burke, A. C., Nelson, C. E., Morgan, B. A. & Tabin, C. Hox genes and the evolution of vertebrate axial morphology. *Development* **121,** 333–346 (1995).
10. Mansfield, J. H. & Abzhanov, A. Hox expression in the American alligator and evolution of archosaurian axial patterning. *J. Exp. Zool. B* **314,** 629–644 (2010).
11. Averof, M. & Akam, M. Hox genes and the diversification of insect and crustacean body plans. *Nature* **376,** 420–423 (1995).
12. Arendt, D. The evolution of cell types in animals: emerging principles from molecular studies. *Nature Rev. Genet.* **9,** 868–882 (2008).
13. Sugino, K. *et al.* Molecular taxonomy of major neuronal classes in the adult mouse forebrain. *Nature Neurosci.* **9,** 99–107 (2006).
14. Palmer, C., Diehn, M., Alizadeh, A. A. & Brown, P. O. Cell-type specific gene expression profiles of leukocytes in human peripheral blood. *BMC Genomics* **7,** 115 (2006).
15. Wagner, G. P. The developmental genetics of homology. *Nature Rev. Genet.* **8,** 473–479 (2007).
16. Young, R. L. & Wagner, G. P. Why ontogenetic homology criteria can be misleading: lessons from digit identity transformations. *J. Exp. Zool. B* **316B,** 165–170 (2011).
17. Robinson, M. D., McCarthy, D. J. & Smyth, G. K. edgeR: a Bioconductor package for differential expression analysis of digital gene expression data. *Bioinformatics* **26,** 139–140 (2010).
18. Welten, M. C., Verbeek, F. J., Meijer, A. H. & Richardson, M. K. Gene expression and digit homology in the chicken embryo wing. *Evol. Dev.* **7,** 18–28 (2005).
19. Tickle, C. Making digit patterns in the vertebrate limb. *Nature Rev. Mol. Cell Biol.* **7,** 45–53 (2006).
20. Vargas, A. O. & Fallon, J. F. Birds have dinosaur wings: The molecular evidence. *J. Exp. Zool. B* **304B,** 86–90 (2005).
21. Vargas, A. O. *et al.* The evolution of HoxD-11 expression in the bird wing: insights from *Alligator mississippiensis*. *PLoS ONE* **3,** e3325 (2008).
22. Uejima, A. *et al.* Anterior shift in gene expression precedes anteriormost digit formation in amniote limbs. *Dev. Growth Differ.* **52,** 223–234 (2010).
23. Montavon, T., Le Garrec, J. F., Kerszberg, M. & Duboule, D. Modeling Hox gene regulation in digits: reverse collinearity and the molecular origin of thumbness. *Genes Dev.* **22,** 346–359 (2008).
24. Firulli, B. A. *et al.* Altered Twist1 and Hand2 dimerization is associated with Saethre-Chotzen syndrome and limb abnormalities. *Nature Genet.* **37,** 373–381 (2005).
25. Zhu, L., Zhou, G., Poole, S. & Belmont, J. W. Characterization of the interactions of human ZIC3 mutants with GLI3. *Hum. Mutat.* **29,** 99–105 (2008).
26. Tzchori, I. *et al.* LIM homeobox transcription factors integrate signaling events that control three-dimensional limb patterning and growth. *Development* **136,** 1375–1385 (2009).
27. Suzuki, R. & Shimodaira, H. Pvclust: an R package for assessing the uncertainty in hierarchical clustering. *Bioinformatics* **22,** 1540–1542 (2006).
28. Wang, L. K. *et al.* DEGseq: an R package for identifying differentially expressed genes from RNA-seq data. *Bioinformatics* **26,** 136–138 (2010).
29. Hargrave, M., Bowles, J. & Koopman, P. *In situ* hybridization of whole-mount embryos. *Methods Mol. Biol.* **326,** 103–113 (2006).
30. Robinson, M. D. & Oshlack, A. A scaling normalization method for differential expression analysis of RNA-seq data. *Genome Biol.* **11,** R25 (2010).

Supplementary Information is linked to the online version of the paper at www.nature.com/nature.

Acknowledgements The authors thank J. Noonan for discussions on this project, K. Cooper for experimental assistance and N. Carriero for read-mapping assistance and C. Tabin for providing us with the Hoxd12 probe. The authors are also grateful for the technical support for this project by the Yale Center for Genomic Analysis. The financial support by the Yale Science Development Fund is gratefully acknowledged.

Author Contributions Z.W. performed the experiments and data analysis and participated in design of the study. R.L.Y., H.X. and G.P.W. participated in data analysis. G.P.W. conceived and designed the study and supervised the work. All authors discussed the results and made substantial contributions to the manuscript.

Author Information All mRNA-seq data are deposited in the Gene Expression Omnibus under accession number GSE28156. Reprints and permissions information is available at www.nature.com/reprints. The authors declare no competing financial interests. Readers are welcome to comment on the online version of this article at www.nature.com/nature. Correspondence and requests for materials should be addressed to G.P.W. (gunter.wagner@yale.edu).

METHODS

Sample collection. Fertilized chicken eggs were obtained from Charles River Laboratories International and incubated between 37.5 and 39 °C at high relative humidity (>50%). To obtain sufficient RNA for transcriptome sequencing, digit samples were collected and pooled from 20 individuals. Previous studies show that digit identity is regulated by the closely posterior interdigital mesoderm and that digit identities of digit I/II and III are not fixed until stages 30 and 29 in the chicken hindlimb[31,32]. Thus, we use digital primordia with their closely posterior interdigital mesoderm to compose a sample for mRNA-seq at stage 28/29, and only the digital ray as a sample at stage 31 (Fig. 1a–d). Collections were performed at two time points during egg incubation to obtain stage 28/29 and stage 31 embryos. Staging is based on Hamburger and Hamilton[33]. Digital primordia with their closely posterior interdigital mesoderm were dissected separately from the forelimb and hindlimb between stages 28 and 29 (stage 28/29; Fig. 1a, b). Digital rays without interdigital tissues were collected from the forelimb and hindlimb at stage 31 (Fig. 1c, d). In both cases, we removed the tissue anterior to the first digital ray of the forelimb. This tissue is thought to be the residual condensation of the ancestral digit I[18].

mRNA-seq. Total RNA was extracted using the RNeasy Mini kit (Qiagen), and treated with DNase I using RNase-Free DNase set (Qiagen). Extracted total RNA of the samples was submitted to Yale Center for Genome Analysis for mRNA sequencing (mRNA-seq) using an Illumina Genome Analyzer. mRNA-Seq 8-Sample Prep kit (Illumina), Standard Cluster Generation kit (Illumina) and Illumina Sequencing kit (Illumina) were used for constructing libraries for single-read sequencing, cluster amplification and final sequencing-by-synthesis. Two flow cells, each containing 8 lanes and 8 samples including the Phi X174 control, were used. Image analysis, base calling, extraction of 34-bp reads, and read counting were performed using the Illumina pipeline.

Sequence alignment, gene counting and normalization. Reads from mRNA-seq data were aligned to Ensembl chicken genome (*Gallus gallus* WASHUC2) using the GERALD module of Illumina CASAVA v1.6 software. After alignment, raw gene counts (gene expression levels) were counted by Illumina CASAVA v1.6 software, and then normalized using the TMM method, which takes RNA composition bias into account, using the edgeR package[17,30]. The normalization factors were calculated by edgeR[17,30] for each library and then the normalized read counts were calculated by the following formula: normalized count = raw count ÷ (library size × normalization factor) × 10^6. The normalized count was directly used for subsequent analyses (see below), and was also divided by the cDNA length to adjust for gene length and then used in the same analysis.

Differential expression analysis. DEGseq[28] packages were used to identify differentially expressed genes between digit I (EFa, LFa, EHa and LHa; Fig. 1a–d) and all the other digits (EFb, EFc, LFb, LFc, EHb, EHc, EHd, LHb, LHc and LHd; Fig. 1a–d), and between LFb and LFc samples (Fig. 1c, d). Function DEGexp was performed to identify differentially expressed genes and the R scripts for using this function are provided in the User's Guide of DEGseq[28]. DEGseq[28] was also used to identify differentially expressed genes between forelimb (EFa, EFb, EFc, LFa, LFb and LFc; Fig. 1a–d) and hindlimb digits (EHa, EHb, EHc, EHd, LHa, LHb, LHc and LHd; Fig. 1a–d), and these genes were removed from the input data for the MDS plot (see below). Owing to the underestimate of the true variability (resulting from pooling individuals), more differentially expressed genes may be removed, which actually makes the downstream approach (MDS plot) conservative. A gene is considered significantly differentially expressed when the *Q*-value (adjusted *P* value for multiple testing) is lower than 0.05 (ref. 34).

MDS plot. The MDS plot is conducted by the edgeR package[17]. The input data are normalized read counts of 5,813 genes after removing genes that are significantly differentially expressed between forelimb digits and hindlimb digits. The distance between each pair of samples in the output figure is the square root of the common dispersion for the top 100 genes that best distinguish that pair of samples[17]. These top 100 genes are selected according to the tagwise dispersion of all the samples[17].

Cluster analysis and heat map of correlation. We produced two sets of data from the normalized data by different methods. The two data sets are separately used for hierarchical clustering and calculating either Pearson's correlation coefficient or Spearman's rank correlation coefficient. The first method considers the mRNA-seq data to follow a Poisson distribution and calculates the square root values of the normalized data (the canonical variance-stabilizing transformation for Poisson). To calculate the input data, the 14 samples are divided into four groups: group 1 (EFa, EFb and EFc), group 2 (EHa, EHb, EHc and EHd), group 3 (LFa, LFb and LFc) and group 4 (LHa, LHb, LHc and LHc) depending on developmental stages and forelimb/hindlimb. A distance is calculated by subtracting the mean of square root values of a group (for example, group 1: all the forelimb digits at stage 28/29) from each square root value of a sample (for example, EFa). The distance matrix is used for clustering and calculating the correlation coefficient between samples.

The second method considers that the normal distribution, with mean λ and variance λ (standard deviation: the square root of λ), is an approximation to the Poisson distribution because of large values of λ (in this study, $\lambda \approx 700$). Thus, a standard score (also called *z*-value, *z*-score), which indicates how many standard deviations a datum is above or below the mean, is used for clustering and calculating Pearson's correlation coefficient between samples.

A heat map of correlation coefficients between samples was created by the R Lattice package. Clustering is conducted by pvclust, an R package for hierarchical clustering with *P* values[27]. After bootstrap re-sampling (10,000 iterations), approximately unbiased (AU) *P* value is provided in the output figure. AU *P* value, which is calculated by multiscale bootstrap re-sampling, is a better approximation to unbiased *P* value than bootstrap probability value calculated by ordinary bootstrap re-sampling. Clusters are formed using the average dissimilarity between the samples. An AU *P* value higher than 95% indicates that the cluster is highly supported[27].

Gene Ontology analysis. Gene Ontology analysis is performed by the GOseq package[35], which takes gene length bias into account. We first identify the significantly differentially expressed genes that are driving the clustering by edgeR package[17] and then identify significantly enriched GO categories using a 0.05 cutoff for the false discovery rate. Default parameters and methods in the packages are used.

***In situ* hybridization.** Total RNA was extracted from chicken embryonic limb buds using the RNeasy Mini kit (Qiagen), and treated with DNase I using RNase-Free DNase set (Qiagen). cDNA was synthesized from the total RNA using the High Capacity cDNA Reverse Transcription kit (Applied Biosystems). The whole coding sequence of *Hand2* was amplified using a pair of specifically designed primers (forward primer, 5′-GCGGCGATGAGTCTTGTG-3′; reverse primer, 5′-CTCACTGCTTGAGCTCCAGC-3′; product, 658 bp). Partial coding sequence followed by partial 3′ UTR of *Zic3* was amplified using a pair of primers previously reported but without the additional T7 RNA polymerase promoter sequence (forward primer, 5′-CAGCAAGGACTCCACGAAAAC-3′; reverse primer, 5′-CGACCCCATCAGATGAGAAT-3′; product, 723 bp)[35]. Most of the coding sequence of *Lhx9* (914 bp) was amplified using a pair of primers previously reported[37]. Most of the coding sequence followed by partial 3′ UTR of *Socs2* was amplified using a pair of specifically designed primers (forward primer, 5′-CGTTGCCGAAGCCAAGGAGA-3′; reverse primer, 5′-AGGGATGCGAG CGGGGATAA-3′; product, 624 bp). PCR products were purified using the QIAquick Gel Extraction kit (Qiagen) and cloned into pGEM-T vector (Promega). All the antisense probes were prepared by linearizing the plasmid with NcoI and transcribing with SP6 polymerase, whereas the sense probes were prepared by linearizing the plasmid with SpeI and transcribing with T7 polymerase. The probe of *Hoxd12* was provided by C. Tabin[38]. All of the probes are labelled with digoxigenin (Roche) and hybridized with the chicken embryos at 70 °C. The procedure of ISH followed a previously published protocol[32].

31. Dahn, R. D. & Fallon, J. F. Interdigital regulation of digit identity and homeotic transformation by modulated BMP signaling. *Science* **289,** 438–441 (2000).
32. Suzuki, T., Hasso, S. M. & Fallon, J. F. Unique SMAD1/5/8 activity at the phalanx-forming region determines digit identity. *Proc. Natl Acad. Sci. USA* **105,** 4185–4190 (2008).
33. Hamburger, V. & Hamilton, H. L. A series of normal stages in the development of the chick embryo. *J. Morphol.* **88,** 49–92 (1951).
34. Benjamini, Y. & Hochberg, Y. Controlling the false discovery rate: a practical and powerful approach to multiple testing. *J. R. Stat. Soc. B* **57,** 289–300 (1995).
35. Young, M. D., Wakefield, M. J., Smyth, G. K. & Oshlack, A. Gene ontology analysis for RNA-seq: accounting for selection bias. *Genome Biol.* **11,** R14 (2010).
36. McMahon, A. R. & Merzdorf, C. S. Expression of the *zic1*, *zic2*, *zic3*, and *zic4* genes in early chick embryos. *BMC Res. Notes* **3,** 167 (2010).
37. Abellán, A. *et al.* Olfactory and amygdalar structures of the chicken ventral pallium based on the combinatorial expression patterns of LIM and other developmental regulatory genes. *J. Comp. Neurol.* **516,** 166–186 (2009).
38. Nelson, C. E. *et al.* Analysis of Hox gene expression in the chick limb bud. *Development* **122,** 1449–1466 (1996).